

1 **Title:**

2 Multiomics-assisted characterization of rice-Yellow Stem Borer interaction provides genomic and
3 mechanistic insights into stem borer tolerance in rice

4 **Running title:** Characterization of rice-Yellow Stem Borer interaction

5 **Authors:**

6 Gokulan C. G.¹, Umakanth Bangale², Vishalakshi Balija², Suneel Ballichatla², Gopi Potupureddi²,
7 Prashanth Varma², Nakul Magar², Kartikey J.², Sravan M.², Padmakumari A. P.², Gouri S Laha²,
8 Subba Rao LV², Kalyani M. Barbadikar², Meenakshi Sundaram Raman², Hitendra K. Patel^{1,3}, M
9 Sheshu Madhav^{2,4,*}, Ramesh V. Sonti^{1,5,*}

10 **Affiliation:**

11 ¹CSIR-Centre for Cellular and Molecular Biology, Telangana, India - 500007.

12 ²ICAR-Indian Institute of Rice Research, Telangana, India - 500030.

13 ³Academy of Scientific and Innovative Research, Uttar Pradesh, India - 201002.

14 ⁴Current address: ICAR-Central Tobacco Research Institute, Andhra Pradesh, India - 533105.

15 ⁵Current address: International Centre for Genetic Engineering and Biotechnology, New Delhi, India
16 - 110067

17 *Addresses for correspondence: sheshu24@gmail.com; sonti@ccmb.res.in

18 **ORCiD:**

19 Gokulan C. G.: 0000-0002-4305-2818

20 AP Padmakumari: 0000-0003-2318-2540

21 Hitendra K. Patel: 0009-0003-4016-4739

22 Sheshu Madhav: 0000-0001-6100-5751

23 Ramesh V. Sonti: 0000-0003-4845-0601

24

25 **SUMMARY:**

26 Yellow stem borer (YSB), *Scirpophaga incertulas* (Walker) (Lepidoptera: Crambidae), is a major
27 pest of rice in India, that can lead to 20-60% loss in rice production. Effective management of YSB
28 infestation is challenged by the non-availability of adequate source of resistance and poor
29 understanding of resistance mechanisms, thus necessitating studies for generating resources to breed
30 YSB resistant rice and to understand rice-YSB interaction. In this study, by using bulk-segregant
31 analysis in combination with next-generation sequencing, Quantitative Trait Loci (QTL) intervals in
32 five rice chromosomes were mapped that could be associated with YSB tolerance at vegetative phase
33 in a highly tolerant rice line named SM92. Further, multiple SNP markers that showed significant
34 association with YSB tolerance in rice chromosomes 1, 5, 10, and 12 were developed. RNA-
35 sequencing of the susceptible and tolerant lines revealed multiple genes present in the candidate QTL
36 intervals to be differentially regulated upon YSB infestation. Comparative transcriptome analysis
37 revealed a putative candidate gene that was predicted to encode an alpha-amylase inhibitor. Analysis
38 of the transcriptome and metabolite profiles further revealed a possible link between phenylpropanoid
39 metabolism and YSB tolerance. Taken together, our study provides insights on rice-YSB interaction
40 at genomic, transcriptomic and metabolomic level, thereby facilitating the understanding of tolerance
41 mechanism. Importantly, a promising breeding line and markers for YSB tolerance have been
42 developed that can potentially aid in marker-assisted breeding of YSB resistance among elite rice
43 cultivars.

44 **Keywords:** Rice, Yellow Stem Borer, QTL mapping, Insect resistance, Transcriptomics,
45 Metabolomics, Markers, Plant breeding.

46 **SIGNIFICANCE STATEMENT:**

47 Global rice production is threatened by various pests, among which stem borers pose serious
48 challenges. Hence, understanding the molecular intricacies of rice-stem borer interaction is necessary
49 for effective pest management. Here, we used a multi-omics approach to unravel the mechanisms that
50 might help rice combat yellow stem borer infestation, thus providing insights and scope for
51 developing YSB tolerant rice varieties. To facilitate the latter, we developed markers that co-
52 segregate with tolerance.

53 INTRODUCTION

54 Several pests affect rice cultivation globally and pose serious threats to grain production and
55 quality. Over a hundred pests have been reported to infest rice, of which 15-20 cause severe agro-
56 economic losses (Pathak, 1968; Pathak, 1977). Yield losses caused by insects can vary depending on
57 the insect biotype, severity of the infestation, environmental factors, growth stage and genetic
58 background of the host (Pathak, 1977). Among the major pests of rice, stem borers pose a serious
59 threat as they cause devastating effects on rice production in both temperate and tropical regions.
60 Commonly found stem borers in Asia include yellow stem borer (YSB; *Scirpophaga incertulas*),
61 striped stem borer (SSB; *Chilo suppressalis*), white stem borer, dark-headed stem borer, and pink
62 stem borer. YSB and SSB were the cause of a steady yield loss of an estimated 5%-10% in Asia
63 (M.D. Pathak and Z.R.Khan, 1994). YSB is a predominant pest among other stem borers in the Indian
64 sub-continent (M.D. Pathak and Z.R.Khan, 1994; Gururaj Katti, Chitra Shanker, Padmakumari A.P.,
65 2011). A study in a field condition revealed that YSB infestation explained about 70% variation in
66 the yield (Gangwar *et al.*, 1986). The female moths of YSB lay eggs on the leaf tips. After hatching,
67 the larvae disperse through wind or move downwards and bore into the stem just above the water
68 level. YSB infestation in rice is manifested as different symptoms based on the growth stage of the
69 plants. The larvae of YSB bore into the rice stem at the base and feed on the growing tissue leading
70 to formation of “dead hearts” in vegetative phase and white ears/ white heads in reproductive phase.
71 Both dead hearts and white ears lead to a considerable yield loss as they both directly affect the
72 production of rice by interfering with the number of productive tillers and panicles, respectively
73 (Pathak, 1968; Muralidharan, K. and Pasalu, 2006). However dead heart damage at vegetative phase
74 can be compensated up to 10% (Rubia *et al.*, 1996).

75 The control of stem borers in the field is still challenging and is majorly dependent on timely
76 chemical intervention. The usage of chemicals affects human health, pollutes the ecosystem, and
77 destroys the natural predators of insects and leads to development of resistance to insecticides. Using
78 resistant or tolerant rice cultivars to counter the attack by pests and pathogens is one of the highly
79 recommended practices in pest management. Resistance or tolerance among different cultivars to
80 different species of stem borers has been reported (Heinrichs, Elvis & Medrano, F.G. and Rapusas,
81 1985). It was observed that the resistance of these varieties was primarily due to antibiosis, that is, an
82 antagonistic reaction of rice towards stem borer which is detrimental to the latter (Pathak, 1977). It
83 was found that rice plants can compensate for the damage through the reallocation of metabolites and
84 photosynthates to uninjured stems/tillers and by initiating the production of new tillers (Rubia *et al.*,

85 1996). Compensation was observed to be an effective strategy to tolerate YSB infestation during the
86 vegetative growth stage and not during the reproductive stage. It was proposed that breeding rice lines
87 for tolerance to YSB based on the ability of the varieties to compensate for the YSB-caused injury
88 could be a better approach (Rubia *et al.*, 1996).

89 Taking note of the extent of spread and severity of the insect (Padmakumari AP and Katti G,
90 2018), the necessity for efficient pest management is imperative. Hence, the development of rice lines
91 with YSB tolerance and using such lines for breeding purposes is of primary importance. This study
92 reports the identification of a promising rice line that shows enhanced tolerance to YSB during
93 vegetative phase of the crop. To further characterize the line and identify it as a potential source of
94 tolerance, bulk segregant analysis and QTLseq analysis of the SM92 mapping population was
95 performed. Putative QTL intervals linked to YSB tolerance were identified in five rice chromosomes.
96 Using SNP genotyping of the segregating population, several markers that showed significant
97 association with YSB tolerance were identified. In order to elucidate the mechanism of tolerance,
98 RNA-sequencing of the tolerant and susceptible lines upon YSB infestation was performed. The
99 analysis revealed modulation of phenyl propanoid pathway, lipid transport, and alpha-amylase
100 inhibition could be key pathways involved in YSB tolerance in rice. Metabolite profiling further
101 indicated accumulation of various phenylpropanoid metabolites upon YSB infestation. Overall, this
102 work identified, characterized, and developed resources for YSB tolerance that could be of potential
103 use in rice breeding.

104

105 **RESULTS**

106 **SM92 was identified to be highly tolerant to YSB**

107 A rice line named SM92 (described in Padmakumari A.P et al 2017; Potupureddi et al. 2021) was
108 found to show tolerance to YSB during vegetative stage of growth (Figure 1A). A cut-stem assay was
109 performed to reveal the status of YSB larvae inside the stems of SM and SM92. The results showed
110 a significantly reduced number of live larvae inside the stems of SM92 as compared to that in SM
111 (Figure 1B, C, D). This suggests the possibility of antibiosis mechanism in SM92.

112 **QTL-seq revealed putative genomic intervals linked to YSB tolerance at vegetative phase**

113 Bulk segregant Analysis (BSA) was performed to identify the genomic regions that are associated
114 with YSB tolerance. For this, the mutant line in the M₆ generation (SM92) was crossed with the
115 wildtype line. A segregating population containing 314 F₂ progenies was screened for YSB tolerance
116 in field conditions for dead heart symptoms (Data S1). The phenotypic segregation followed normal
117 distribution suggesting that the trait is governed by Quantitative Trait Loci (QTL; Figure 2A). The
118 tolerant and susceptible DNA bulks as well as the parental DNA were subjected to a high coverage
119 (~40X) of next-generation whole genome sequencing. The obtained raw reads were processed,
120 aligned to the reference genome, and the variants were called. The variants were then used for the
121 QTL-seq analysis to identify the QTL associated with YSB tolerance. QTL-seq analysis was
122 performed using two different parameters, namely delta-SNP-index and G-prime (G'). The analyses
123 overall revealed regions in 5 of the 12 rice chromosomes, namely chromosomes 1, 5, 7, 10, and 12,
124 to be putatively linked to YSB tolerance (Figure 2B, C). In total, 10 QTL intervals were predicted in
125 these 5 chromosomes (Table 1).

126 A comparison between the YSB tolerance QTL intervals and previously reported insect resistance
127 QTL was performed. The QTL intervals identified in this study overlapped with the predicted QTL
128 intervals linked to resistance against rice leaf folder (Chr1; Selvaraju et al., 2007) and BPH (Chr10
129 and Chr12; Sun et al., 2005; Jena et al., 2006) (Table S3). Although these QTL intervals are mapped
130 for insect resistance, there is no further information on the possible genes or their alleles that might
131 be involved in resistance. Also, no markers have been developed from these intervals for application
132 in breeding programmes.

133

134 **A large number of genes in the QTL intervals exhibit variations**

135 The genes that harbor SNPs and that are present in the QTL interval were annotated using Variant
136 Effect Predictor (VEP). There were 25,065 SNPs present in the QTL intervals in all five chromosomes
137 (Figure S1A; Data S2). About 94% of these SNPs were in non-coding regions of the genome (Figure
138 S1B). A total of 1101 genes harbor SNPs which include SNPs in coding (UTRs and exonic) and/or
139 non-coding (upstream, downstream, and intronic) regions. Genes harboring SNPs in their coding
140 regions were 459 in number and 34 among them harbored SNPs that were predicted to be deleterious
141 (Data S3). Over-representation analysis of the genes that harbor mutations in the coding sequences
142 revealed a significant enrichment of laccase-encoding genes, that are involved in
143 phenylpropanoid/lignin metabolism (Figure S1C).

144 **Marker-Trait Association Analysis revealed markers exhibiting significant association with**
145 **YSB tolerance at vegetative phase**

146 A set of fifty SNPs were selected as markers for genotyping the F₂ individuals using Kompetitive
147 Allele Specific PCR (KASPTM, LGC Genomics, UK; Data S4, S5). These SNPs were selected based
148 on their effect on the genes that harbor them, the genomic distance between the preceding and the
149 following SNP in such a way that the distance between the two markers is less than 250-300 kbp.
150 KASP assay was performed from the F₂ plants showing extreme as well as intermediate phenotypes
151 (Data S6). Further, a marker-trait association analysis was carried out to identify the markers that are
152 significantly associated with the phenotype (Data S7). The KASP-based genotyping revealed a
153 significant ($P<0.05$) association of fourteen alleles from chromosomes 1, 5, 10, and 12 with YSB
154 tolerance in the F₂ individuals (Table 2). Each of the regions was calculated to explain about 5% to
155 9% phenotype variation observed in the F₂ progenies.

156 **YSB infestation causes an extensive transcriptional reprogramming**

157 Transcriptomics-based characterization of rice-YSB interaction was performed to understand the
158 possible mechanism of tolerance to YSB. For this, RNA sequencing (RNA-seq) was performed on
159 RNA isolated from the stem tissues of SM and SM92, with and without YSB infestation (3 days post
160 infestation). The analysis of RNA-seq data showed several differentially expressed genes (DEGs)
161 with overlapping and unique DEGs between SM and SM92 (Figure 3A, B; Data S8, S9). The number
162 of DEGs was slightly more in SM (n=1950) when compared to SM92 (n=1857). Also, SM92 had a
163 lesser number of downregulated genes than SM. Overall, only 13.7% of the DEGs were common
164 between SM and SM92, suggesting a contrasting transcriptional reprogramming occurring in tolerant
165 and susceptible lines upon YSB infestation.

166 Gene ontology (GO) and pathway enrichment analysis of the DEGs revealed the similarities and
167 differences between SM and SM92 in terms of their transcriptomics response to YSB infestation
168 (Figure 3C, D). Specifically, YSB-induced genes in SM92 were enriched in phenylpropanoid
169 metabolism, alpha-amylase inhibitors/lipid transfer protein and glycoside hydrolases (Figure 3D). An
170 in-depth analysis using MapMan revealed genes belonging to the GO term ribosome biogenesis were
171 exclusively downregulated in SM (Figure S2A). The categories consisting of genes involved in the
172 metabolism of simple phenols, lignin and lignans showed a striking difference between SM and
173 SM92, wherein these genes were majorly upregulated in SM92 (Figure S2B).

174 **Phenylpropanoid pathway genes show remarkably contrasting expression pattern at**
175 **vegetative phase infestation in tolerant and susceptible lines**

176 Genes involved in the biosynthesis of phenylpropanoids showed a remarkable upregulation in SM92
177 while some of the genes were downregulated in SM (Figure 3D; Figure S3). The Phenylpropanoid
178 Pathway (PPP) is an important secondary metabolism pathway that is essential for normal plant
179 growth, development and defense against various pests and pathogens (Dong and Lin, 2021). PPP
180 leads to the production of various types of lignin and lignin derivatives. In line with this, overall,
181 thirteen *laccase*-encoding genes, that are predicted to be involved in lignin metabolism, were
182 upregulated in SM92 upon YSB infestation. Markedly, five of the thirteen *laccase* genes are present
183 within the chromosome 1 QTL interval (Table S4). Further analysis revealed that cumulatively 118
184 genes that are in the QTL intervals are differentially expressed in SM and SM92 upon YSB infestation
185 (Data S10). A deeper look into these genes indicated lignin metabolism-related genes, *laccases* (n=5),
186 to be enriched among the genes upregulated exclusively in SM92 (Figure S4A). Promoter analysis of
187 the five *laccase* genes revealed the presence of tandem CATG palindromic motif (CATGCATG) in
188 the promoters of all five genes (Fig S4B). Further analysis indicated a significant overlap between
189 the observed motif and the binding element of a B3-domain containing transcription factor (Figure
190 S4C). It could hence be speculated that a common mode of regulation might be acting on these *laccase*
191 genes in SM92, probably mediated by a B3-domain containing transcription factor.

192 **Comparative analysis suggests putative candidate genes for stem borer tolerance in rice**

193 A comparative transcriptomics analysis was performed between the data generated in this study and
194 a previously published data where rice lines with varying degree of resistance to striped stem borer
195 (SSB) were infested with SSB (Wang *et al.*, 2018). It was observed that 527 genes were commonly
196 upregulated by SSB and YSB in the respective tolerant lines (Figure 4A; Data S11). A gene set
197 enrichment analysis revealed that genes annotated as alpha-amylase inhibitors/lipid transfer protein,

198 carbohydrate metabolism, and cell wall-related genes were significantly enriched (Figure 4B). A
199 striking observation was that the highest upregulated gene in SM92 upon YSB infestation –
200 *OsLTPL146*, a Lipid Transfer Protein-like (LTPL) gene – is present within the mapped QTL interval
201 in Chromosome 10. In addition, the same gene was significantly downregulated in SM. *OsLTPL146*
202 exhibited a similar expression pattern upon SSB infestation as well. That is, *OsLTPL146* was
203 upregulated in a resistant cultivar and downregulated in a susceptible cultivar upon SSB infestation
204 (Figure 4C). Interestingly, it was also observed that twenty-five lipid-metabolism/transport related
205 genes majorly including *LTPL* class of genes were upregulated in SM92 upon YSB infestation, while
206 only five genes showed differential expression in SM (Figure S5A). Other lipid/fatty-acid metabolism
207 related genes that are involved in cutin, suberine, and wax synthesis were also exclusively upregulated
208 in SM92 (Figure S6). Another unique expression pattern observed was that of the glutathione
209 metabolism genes consisting of the Phi and Tau classes of *glutathione transferases (GSTs)*. These
210 genes were exclusively upregulated in SM92 post YSB attack (Figure S6).

211 As mentioned above, twenty-five enriched genes belonged to the lipid metabolism/transport category.
212 Of the twenty-five genes, twenty-two genes were annotated as “Protease inhibitor/seed storage/LTP
213 family protein precursor”. To elucidate the actual biochemical properties of these gene products, the
214 structures of all the twenty-five protein sequences were predicted using AlphaFold2 and their
215 structural homologues were identified. The results suggest that fifteen genes likely encode lipid
216 transfer proteins as their structures were homologous to characterized lipid transfer proteins from
217 various organisms, five gene products were homologous to alpha-amylase inhibitors and of the
218 remaining five genes, one coded for a lyase, one for a phospholipase D, one for annexin and the
219 structures could not be predicted for the other two gene products (Figure S5B).

220 Notably, structure prediction analysis suggests that the predicted structure of *OsLTPL146* is
221 homologous to an alpha-amylase inhibitor whose structure is experimentally solved. This result
222 indicates that *OsLTPL146* – the highest upregulated gene in SM92 upon YSB infestation – likely
223 encodes an alpha-amylase inhibitor (Figure 4D). Further, owing to the difference in the expression
224 pattern of *OsLTPL146* in SM and SM92, the promoter sequence of *OsLTPL146* in SM and SM92
225 were compared. The alignment revealed considerable variations in the promoter and 5' untranslated
226 region (UTR) of the gene between SM and SM92 in certain known cis-elements. The variations
227 included single nucleotide polymorphisms, small insertions, and deletions (Figure S7). Whether the
228 variations in the promoter/regulatory sequence of *OsLTPL146* are involved in the YSB-mediated
229 induction of the transcript and/or YSB tolerance is another avenue for further research. Taken

230 together, detailed investigation of OsLTPL146 promoter variation and protein biochemistry could
231 reveal its role in stem borer resistance.

232 **Levels of a few phenylpropanoid pathway metabolites are altered upon YSB infestation**

233 An untargeted metabolite profiling of sheath samples that were either uninfested or infested with YSB
234 larvae was performed to gain insights into the mechanism of tolerance to YSB. Over 1000 metabolites
235 were identified in all the tested conditions (Data S12, and S13). The overall profile indicated a
236 difference in the metabolite levels between uninfested SM and SM92 plants. However, YSB
237 infestation seems to result in highly comparable metabolite profile in both SM and SM92 (Figure
238 5A). Further, the levels of phenylpropanoid pathway (PPP) associated metabolites were analysed
239 specifically, as the RNA-seq data indicated an upregulation of genes associated with the pathway.
240 The results showed the presence of 27, and 25 PPP metabolites in SM and SM92 samples, respectively
241 (Figure S8). Four of the PPP metabolites including 5-O-Caffeoylshikimic acid, Coniferyl acetate,
242 Caffeate, and L-Phenylalanine exhibited significant differential accumulation in SM and/or SM92
243 upon YSB infestation when compared to uninfested samples (Figure 5B). YSB infestation resulted in
244 increased levels of 5-O-Caffeoylshikimic acid and Coniferyl acetate in both SM and SM92. On the
245 other hand, Caffeate and L-Phenylalanine exhibited significantly reduced accumulation in SM92
246 upon YSB infestation. Owing to the variation among the samples, difference in the levels of other
247 metabolites could not be reliably identified. Targeted analysis of PPP metabolites could provide a
248 better understanding of the regulation of the pathway with respect to YSB infestation.

249 **DISCUSSION**

250 Stem borers cause maximum yield loss among all the insects that attack rice in India (Savary *et al.*,
251 2019). Complete resistance to stem borers in nature is scarce and unidentified yet. Being a
252 monophagous pest, it feeds only on rice plants and perpetuates. As a borer, by nature of its feeding
253 habit it must feed on the plant for its survival. The damage occurs in the process of entering the plant
254 and therefore some extent of damage is inevitable. Hence, the dependance on chemical insecticides
255 prevail despite their negative impact on health and the ecosystem (Su *et al.*, 2014). Most stem borer
256 tolerant varieties of rice exhibit compensation and antibiosis traits (Rubia *et al.*, 1996). However, the
257 exact mechanism of tolerance and the molecular players involved are unknown.

258 The advent of bulk segregant analysis and next-generation sequencing methods have accelerated QTL
259 identification and gene mapping for the traits of interest. This study identified a rice line, named
260 SM92, that is highly tolerant to YSB. Screening the F₂ population, generated through bi-parental
261 mating, at vegetative phase revealed that YSB tolerance to be a quantitative trait. Therefore, the
262 segregants with extreme phenotypes were used for preparing tolerant and susceptible DNA bulks and
263 were subjected to high-coverage sequencing. Analysis of the sequence data using QTL-seq pipeline
264 indicated the presence of QTL intervals in five rice chromosomes that are putatively linked to YSB
265 tolerance, thus validating the observed segregation pattern. Notably, three of the identified genomic
266 regions were found to be overlapping with known insect resistance QTL intervals (Table S3). That is
267 the Chr1 QTL was partly overlapping with a previously identified rice leaf folder resistance QTL
268 whereas the Chr10 and Chr12 QTL intervals partly overlap with BPH resistance QTL. This
269 observation suggests that the identified genomic intervals are of potential importance in insect
270 resistance/tolerance and are likely to contain genes/alleles that are part of the insect
271 resistance/tolerance mechanism of rice. The QTL mapping data indicated that SM alleles contribute
272 to tolerance arising from Chromosome 1 QTL interval whereas SM92 alleles contribute to tolerance
273 arising from other intervals (Figure 2B). Further analysis indicated that *laccase* genes, involved in
274 lignin metabolism, are overrepresented in the QTL intervals.

275 **Laccases and plant defense**

276 Laccase (LAC; EC1.10.3.2) belongs to a multi-copper oxidase family of enzymes that play a crucial
277 role in plant development and stress responses (Yu *et al.*, 2021). Various studies have identified the
278 multi-faceted roles of laccases in plants that include cell wall elongation, secondary cell wall
279 formation, lignification, pigmentation, flavonoid biosynthesis, metal ion stress, and seed setting.
280 Laccases are involved in catalyzing the polymerization of lignin monomers in the apoplast (Zhao *et*
10

281 *al.*, 2013). Lignin, being a component of the secondary cell wall, plays important roles in protecting
282 cells from pathogens. Previous studies have established a positive correlation between lignin
283 accumulation and resistance to bacterial and fungal infections (Lee *et al.*, 2019; Peltier *et al.*, 2009).
284 Previous studies have also associated the levels of lignin pathway precursors including
285 hydroxycinnamic acid positively with resistance to stem borers (Santiago *et al.*, 2013; Malvar *et al.*,
286 2008). A study in maize showed a positive correlation between levels of phenylpropanoids including
287 *p*-coumarate and syringyl lignin to Mediterranean Corn Borer resistance (Gesteiro *et al.*, 2021). Our
288 transcriptome profiling indicated thirteen *laccase* genes to be significantly upregulated in SM92 upon
289 YSB infestation. Additionally, some of the genes involved in the phenylpropanoid metabolism
290 pathway exhibited a strikingly contrast expression pattern in SM (downregulated) and SM92
291 (upregulated) upon YSB infestation. Notably, five of the thirteen *laccase* genes are in the identified
292 QTL intervals in Chromosomes 1. It was also noted that some of the phenylpropanoid pathway genes
293 were downregulated in SM, the susceptible line (Figure S3). Together, the data suggest a likely
294 involvement of lignin metabolism in conferring tolerance to YSB. Although previous studies have
295 pointed out a generic role of laccases in pathogen/pest resistance, our study has provided promising
296 candidate genes that can be studied further to understand the mechanism of tolerance at molecular
297 level.

298 **Ribosomal proteins as potential candidates to understand plant defense mechanisms**

299 On examining the gene enrichment in the susceptible interaction, a remarkable number of genes that
300 code for ribosomal subunit proteins (RPs – Ribosomal proteins) were found to be significantly
301 downregulated. Both the large and small subunit protein-encoding genes were highly downregulated.
302 Previous studies have pointed out that RPs possess moonlighting functions. Such extra-ribosomal
303 functions of RPs include RNA-binding and promoting/preventing translation, role in apoptosis, cell-
304 cycle regulation, and stress resilience in prokaryotes as well as eukaryotes (Wool, 1996; Weisberg,
305 2008; Warner and McIntosh, 2009; Trautmann and Ramsey, 2022). In plants, two RPs viz. RPL12
306 (Ribosomal Protein Large subunit 12) and RPL19 in *Nicotiana benthamiana* and *Arabidopsis*
307 *thaliana* were shown to be important for non-host resistance as the mutants exhibited delayed
308 hypersensitive response to non-host pathogens (Nagaraj *et al.*, 2016; Ramu *et al.*, 2020). A targeted
309 transcriptome profiling of thirty-four large subunit genes indicated that they are highly stress
310 responsive. The genes were either upregulated or downregulated depending on the nature of the stress.
311 Infection of rice plants with the bacterial blight pathogen caused upregulation of the majority of the
312 tested RPs (Moin *et al.*, 2016). Downy mildew infection in grapevine resulted in accumulation of RPs

313 during the early timepoints post-infection (Santos *et al.*, 2020). However, our data revealed a
314 significant downregulation of ribosomal protein-coding genes. This could be an energy-conserving
315 strategy that the host deploys to enhance defense against insect attack. But it is also possible that
316 reduced expression of RPs is a consequence of the mechanisms that the pest uses to suppress defense,
317 and this ultimately results in the host succumbing to the attack. It is noteworthy that the tolerant line
318 did not show any alteration in the expression of RP-encoding genes (Figure S2A), thus suggesting
319 susceptibility being a consequence of RP gene downregulation. Further studies that follow the
320 expression pattern of RP-encoding genes at different time points post infestation can provide a clearer
321 picture of the role of RPs in rice-stem borer interaction.

322 **Insights gained through structure prediction analysis**

323 Another striking observation from the transcriptomics data was the differential expression of
324 approximately twenty genes that were annotated as Lipid transfer-like proteins (LTPLs)/Protease
325 inhibitors (PIs). One of the genes *OsLTPL146* showed the highest upregulation ($\log_2\text{FC} > 10$) upon
326 YSB infestation in the tolerant line while it was downregulated in the susceptible line. Importantly,
327 *OsLTPL146* is located in the Chromosome 10 QTL interval, suggesting a possible link between the
328 expression of the gene and YSB tolerance at vegetative phase. A similar pattern of expression was
329 observed for *OsLTPL146* in an independent transcriptomics study performed in rice upon striped stem
330 borer infestation (Wang *et al.*, 2018). Owing to the high sequence similarity between LTPs and PIs,
331 based on the annotation and sequence alone it is hard to predict the biochemical function of their gene
332 products. Hence, the recently developed, artificial intelligence-based AlphaFold2 was used to predict
333 the structure of the differentially expressed LTPLs (Jumper *et al.*, 2021). The results indicated that
334 fifteen out of the twenty LTPLs exhibit structural homology to lipid transfer proteins while the rest
335 five were homologous to alpha-amylase inhibitors. The presence of proteins of different classes
336 suggest that multiple modes of tolerance are likely in action including protease inhibition, lipid
337 transfer, and alpha-amylase inhibition.

338 Lipid transfer proteins (LTP and LTP-like (LTPL) proteins) have been associated with pathogen
339 resistance, plant development, abiotic stress development, and cuticular wax metabolism among
340 others (Gao *et al.*, 2022). LTPs are small proteins that bind to lipids and aid in their transport across
341 cellular compartments (Salminen *et al.*, 2016). Multiple rice LTPs/LTPLs have been associated with
342 pollen development, tolerance to abiotic stress such as drought, and plant development (Gao *et al.*,
343 2022). *OsLTP5* was found to be induced by cutin monomers, abscisic acid, and salicylic acid (Kim
344 *et al.*, 2008). Cutin monomers possess a defense elicitation property against a potential invasion

345 (Schweizer *et al.*, 1996; Fauth *et al.*, 1998; Kolattukudy *et al.*, 1995). Class I LTPs were identified to
346 be induced upon infection by the blast fungus, *Magnaporthe oryzae* (Tae *et al.*, 2006). The damage
347 caused by fungus and chewing insects results in cuticle damage which in turn leads to the generation
348 of cutin monomers that subsequently activate defense signaling such as accumulation of H₂O₂ (Fauth
349 *et al.*, 1998). Moreover, our transcriptome analysis also revealed enrichment of genes involved in
350 cutin/wax biosynthesis to be upregulated in SM92 upon YSB infestation, suggesting a possible
351 production of cutin and/or reorganization of the cuticle being associated with YSB tolerance.

352 Alpha-amylase inhibitors (AAIs) belong to multi-family proteins that interact with and inhibit alpha-
353 amylase enzymes (Franco *et al.*, 2002; Oneda *et al.*, 2004). Alpha amylases are important digestive
354 enzymes that help in the digestion of plant-derived starch/amylose that are ingested by the insects
355 (Lage, 2018). The evolutionary arms race between plants and pests has resulted in the evolution of
356 AAIs that inhibit alpha-amylase activity in the insect gut and thus negatively impacts insect survival
357 (Franco *et al.*, 2002).

358 **Multi-layered mechanisms to counter stem borer infestation in rice**

359 Studies so far have identified such tolerance-associated mechanisms individually in different
360 plants/varieties. But our observations in combination with other reports in the literature suggest a
361 multimodal mechanism of tolerance to YSB in SM92. Our results suggest that the striking
362 upregulation of multiple Lipid Transfer Protein like genes and alpha-amylase inhibitor genes in SM92
363 is potentially linked to YSB tolerance in a manner that is either dependent on or independent of
364 wax/cuticle damage. Upregulation of a considerable number of lipid transfer protein-like (LTPL)
365 genes indicates a possibility of major alteration in the lipid composition of the cells. The upregulation
366 of cutin/wax synthesis genes in combination with *LTPLs* provides a reasonable indication of the
367 involvement of lipid translocation during insect attack as a plant defense strategy. More studies on
368 this can provide novel insights into plant defense signaling and mechanisms involving lipid moieties.
369 Also, future studies directed towards OsLTPL146 and its amylase inhibition activity could provide a
370 native source of alpha-amylase inhibition thereby eliminating the need for a source of foreign origin.

371 Additionally, the upregulation of phenylpropanoid metabolism genes and laccases adds one more
372 layer to the complex mechanism of YSB tolerance in SM92. The presence of signature motif in the
373 promoter sequence of similarly regulated *laccases* suggests a common regulatory network that might
374 control the expression of lignin metabolism genes in SM92 upon YSB infestation. Therefore, SM92
375 is a very promising line for gaining insights into fundamental resistance mechanisms as well as for
376 breeding programmes to introgress YSB tolerance into breeding lines. The former can be
13

377 accomplished by studying the candidate genes from this study based on QTL-seq and transcriptomics
378 results, while the latter has been facilitated by the markers that were identified to be significantly
379 associated with tolerance.

380 **Breeding for YSB tolerance**

381 Marker-assisted breeding is a viable option for introgressing traits from one crop variety to another.
382 In this regard, several SNP markers have been identified in this study that span the QTL intervals in
383 four different chromosomes. Notably, the Chr10 QTL interval was fine mapped to a ~180kb region
384 with five linked SNP markers. On the other hand, a few markers have been identified to be linked to
385 YSB tolerance in Chr1, Chr5, and Chr12 QTL intervals. Further mapping studies and marker-trait
386 association analyses using high density markers could help in fine mapping the QTL intervals thereby
387 providing additional markers with tight linkage/association to YSB tolerance.

388 Overall, our study provides important insights at genomic, transcriptomic, and metabolomic levels to
389 uncover the mechanism of tolerance to stem borers in rice. Stem borers, one of the major group of
390 pests affecting global rice production, in combination with changing and erratic climatic conditions,
391 pose a serious threat to food security. Knowledge from this study would aid in orienting future
392 research to better understand the mechanisms as well as provide additional gene targets to breed stem
393 borer resistance in rice and possibly in other related crops.

394 **EXPERIMENTAL PROCEDURES**

395 **Plant materials and Insect**

396 Plant materials used for this study include the cultivar Samba Mahsuri (SM) and the EMS mutant line
397 named SM92. SM92 is registered as a germplasm at ICAR-National Bureau of Plant Genetic
398 Resources (National Identity: IC646828). Yellow Stem Borer (YSB; *S. incertulas*) moths were
399 collected from the rice field and were released for egg laying on rice plants. The neonate larvae
400 emerging from the egg masses were used for infestation of the mutant lines, F₂, and F_{2:3} progeny
401 under field conditions by releasing 2 neonate larvae per tiller at the maximum tillering phase (Bentur
402 JS *et al.*, 2011; Padmakumari AP and Katti G, 2018). The phenotype was scored when the dead heart
403 symptoms were apparent on the susceptible cultivar (IRRI, 2014). All the YSB screening activities
404 were conducted in the greenhouse and/or rice field facility of ICAR – Indian Institute of Rice
405 Research, Hyderabad, India (17.32°N, 78.39°E).

406 **Cut-stem assay**

407 Cut stem insect bioassays were carried out at the ICAR- IIRR. At vegetative phase, stem cuttings
408 were collected from healthy tillers of both SM and SM92. The stems were cut into 4-5 cm long pieces
409 and placed on Petri plates containing Whatman paper moistened with benzimidazole (75 mg/L).
410 Freshly hatched neonate YSB larvae were then released onto each cut stem at 5 larvae/stem. The
411 plates were kept in an incubator at 27±2°C. After 4 days, the plates were opened, and the stems were
412 dissected carefully under a microscope. Before dissection, the stem pieces were observed for the
413 presence of feeding holes. Upon dissection, the stems were observed for feeding injury and for the
414 number of dead/surviving larvae were counted.

415 **Bulk segregant Analysis and sequencing**

416 For mapping the genomic region(s) associated with YSB tolerance, bulk segregant analysis (BSA)
417 followed by next-generation sequencing and QTL-seq analysis was performed as described earlier
418 (Takagi *et al.*, 2013; Mansfeld and Grumet, 2018). A cross was made between SM (WT; recipient)
419 and SM92 (Mutant; donor). The F₁ plants were confirmed for hybridity and advanced to F₂ generation
420 comprising 314 plants. The F₂ progenies and the parental lines were screened during the vegetative
421 growth phase. The plants were scored based on the percentage of dead heart as recommended by the
422 Standard Evaluation System of Rice (IRRI, 2014). F₂ plants showing the extreme phenotypes i.e.,
423 tolerance (n=21) and susceptibility (n=23) to YSB were selected to constitute the tolerant and
424 susceptible bulks, respectively, after confirming the phenotypes of the F_{2:3} lines. DNA from the bulk
425 constituents and parents were isolated using the CTAB method and quantified using Qubit™ High-
15

426 Sensitivity dsDNA Assay in a Qubit™ 4 fluorometer (Thermo Fisher Scientific, USA). The DNA
427 quality was assessed on 0.8% agarose gel through electrophoresis. Equal concentrations of DNA from
428 the tolerant and susceptible plants were bulked separately. 1 µg DNA from all the samples was used
429 to prepare sequencing libraries with TruSeq Nano DNA HT Sample Preparation Kit (Illumina, USA)
430 and qualified libraries were sequenced on the Illumina HiSeq2500 platform to obtain 2x150 bp reads
431 at approximately 40x coverage. The library preparation and sequencing were outsourced to Nucleome
432 Informatics Private Limited, Hyderabad, India.

433 **Sequencing analysis and gene mapping**

434 Raw reads were obtained from the service provider and processed using *FastQC* to assess the quality.
435 The reads were then used for aligning against the reference genome (Nipponbare) using *BWA mem*.
436 The initial alignment (.bam) files were sorted, and duplicates were removed using *Samtools*. The
437 analysis-ready bam files were used for calling variants using *freebayes* and the variants were filtered
438 and processed using *VCFtools* and *bcftools*. The variants were filtered to retain only Single
439 Nucleotide Polymorphisms (SNPs) with a mapping quality greater than 30, a minimum and the
440 maximum depth of 10 and 200, respectively. The filtered SNPs were then provided as input to the R
441 language-based QTL mapping tool called *QTLseqr* with default filtering criteria and 0.5 Mb window
442 size. The *QTLseqr* identifies QTL intervals by calculating two parameters namely, Delta-SNP-index
443 and the G' statistics (Mansfeld and Grumet, 2018; Magwene *et al.*, 2011). The DNA sequence and
444 analysis statistics are provided in Table S1.

445 **SNP annotation and analyses**

446 Information of the putative QTL intervals obtained from the QTL-seq analysis was used to obtain the
447 variations in the intervals. *Bedtools* (Quinlan and Hall, 2010) was used to extract the SNPs in the
448 QTL interval from the whole genome variant file. The QTL SNPs were then annotated using *Variant*
449 *Effect Predictor* (VEP) to identify the effect of the SNPs on the genome. Microsoft Excel was used
450 for further analyses like segregating the SNPs based on their effects.

451 **Marker development and validation**

452 SNPs having a high impact on the associated genes were chosen based on the effect (non-sense
453 mutations) and SIFT score (missense mutations causing intolerable amino acid changes) provided by
454 VEP. The presence and absence of selected SNPs in SM92 (mutant line) and SM (the wildtype line),
455 respectively, were confirmed through Sanger's sequencing. A total of 50 SNPs (42 from the QTL
456 intervals and 8 from the rest of the genome) were finally selected for developing Kompetitive Allele
457 Specific PCR (KASP™) assays (LGC Genomics, UK). The F₂ individuals derived from SM92 X SM

458 cross were genotyped using KASP assays for all 50 SNPs in the ABI ViiA7 RT-PCR System or Bio-
459 Rad CFX384 system. The genotyping was performed in a 5 μ l reaction per assay under conditions
460 recommended by the manufacturer. KASP reaction condition was as follows: 94 °C - 15 minutes; 10
461 cycles of 94°C for 20 seconds and 61-55°C for 1 minute (touch-down of 0.6°C/cycle); 26 cycles of
462 94°C for 20 seconds and 55°C for 1 minute. TASSEL was used to statistically assess the association
463 between the genotypes and YSB tolerance.

464 **RNA sequencing and analysis**

465 SM and SM92 plants were infested with YSB larvae during the tillering stage. Stem samples were
466 collected from the infested stems an area 1 cm on either side of the larval entry hole 3 days after
467 release of larvae. Also, uninfested stem samples were collected as a control. All the samples were
468 collected as duplicates. The samples were flash-frozen immediately after collection and stored at -
469 80°C until further processing. RNA was isolated from the samples using RNeasy Plant RNA Isolation
470 Kit (Qiagen, Germany) with on-column DNA digestion using RNase-Free DNase Set (Qiagen,
471 Germany). Purified RNA was quantified using Qubit™ RNA HS Assay Kit (Thermo Fisher
472 Scientific, USA). RNA integrity was assessed using agarose gel electrophoresis and BioAnalyzer
473 2100 (Agilent Technologies, USA). 1 μ g of total RNA samples was used for library preparation for
474 each sample using the Illumina TruSeq Stranded Total RNA with Ribo-Zero Plant (Illumina, USA).
475 Sequencing was performed on Illumina's NovaSeq6000 platform with cycling conditions to obtain
476 2x100bp reads on an S2 flowcell to obtain ~70 million reads per sample. The RNA sequence statistics
477 are provided in Table S2. Library preparation and sequencing were performed in the NGS facility of
478 CSIR-CCMB, Hyderabad.

479 The raw data was obtained, and the quality was assessed using *FastQC*. Adapters and low-quality
480 reads were trimmed using *Trim Galore!* (Krueger). *RNA-STAR* was used to align the trimmed reads
481 to the rice genome (MSU Rice Genome Annotation Project - version 7) (Dobin *et al.*, 2013). Reads
482 that mapped to the genes were quantified using *featureCounts* (Liao *et al.*, 2014). Differential gene
483 expression was obtained using the R library *DEseq2* (Love *et al.*, 2014). Genes with a false discovery
484 rate ≤ 0.05 and \log_2 fold change ≤ -2 or ≥ 2 were considered differentially expressed genes (DEGs).
485 For gene ontology, and pathway analyses of the DEGs, tools including gProfiler, ShinyGO, and
486 MapMan were used (Thimm *et al.*, 2004). *Venny* was used for generating Venn diagrams (Oliveros,
487 2007).

488 **Structure prediction and homology search**

489 Amino acid sequences of the DEGs classified under the Lipid Transport/Metabolism category were
490 retrieved from RAPDB ([RAP-DB](#); Sakai *et al.*, 2013; Kawahara *et al.*, 2013). The sequences were
491 subjected to structure prediction using ColabFold ([AlphaFold2.ipynb - Colaboratory](#)) which uses the
492 AlphaFold2 algorithm to predict 3D structure models of proteins (Mirdita *et al.*, 2022). In order to
493 identify the structural homologues of the predicted structures, a structural homology search was
494 performed using the PDB search option of DALI server ([Dali server](#); Holm, 2022). Multiple sequence
495 alignment of protein sequences and the phylogenetic tree were generated using [Clustal Omega](#)
496 (Sievers *et al.*, 2011; Goujon *et al.*, 2010). The phylogenetic tree visualization and annotation were
497 performed using [iTOL](#) (Letunic and Bork, 2021).

498 **Metabolite profiling and analysis**

499 SM and SM92 plants were infested with YSB larvae during the tillering stage. Stem samples were
500 collected from the infested stems an area 1 cm on either side of the larval entry hole 3 days after
501 release of larvae. Also, uninfested stem samples were collected as a control. All the samples were
502 collected in triplicates. The samples were flash-frozen immediately after collection and stored at -
503 80°C until further processing. Further, the frozen samples were lyophilized thoroughly, weighed, and
504 30 mg of the lyophilized samples were powdered. Metabolites were extracted in 1ml of 80% methanol
505 at 30°C for 30 minutes in shaking condition before centrifuging the samples at 14000rpm for 5
506 minutes. The supernatant was filtered through 0.22µm membrane. The extracts (10µl each) were
507 analysed by the Shimadzu Prominence HPLC coupled with Shimadzu triple quadrupole LCMS-8045
508 mass spectrometer (Shimadzu Corporation, Kyoto, Japan). HPLC was performed with a CLC0181
509 column (Shimpack Gist C18 75*4.0mm, 3µm) with a runtime of 50 minutes at a flow rate of
510 0.8mL/minute and column temperature of 30°C. Mobile phases used for HPLC include 0.04% (v/v)
511 acetic acid in water and 100% acetonitrile. The electrospray ionization (ESI)-MS analysis was
512 performed in both positive and negative ion modes. Full-scan mass spectra were acquired over a mass
513 range of m/z 50–2000. The sample extraction and metabolite profiling were outsourced to Novogene
514 Technologies Pvt. Ltd., Hyderabad, India.

515 The raw intensity data of the detected metabolites was analysed using the one factor statistical
516 analysis module of MetaboAnalyst 5.0 using KEGG compound identifiers (Pang *et al.*, 2021). The
517 data was normalized using quantile normalization method, log-transformed, and scaled using the
518 auto-scaling option. The results were downloaded and further processed in Microsoft Excel.

519 **DATA AVAILABILITY**

520 SM and SM92 parent whole genome sequences are deposited in NCBI-SRA under the accession
521 PRJNA658718. The F₂ bulk DNA data are present under the accession PRJNA972670.

522 **AUTHOR CONTRIBUTIONS**

523 Conceptualisation - RVS, MSM, HKP, and PAP. Investigation - GCG (QTL-seq, RNA-seq,
524 metabolomics analyses and KASP genotyping); UB, VB, SB, PAP (YSB rearing, F₂ population
525 generation, and screening of rice plants); PV, NM, KJ, SM, PAP (screening of plants in various
526 seasons). Assessment and supervision of the work - GSL, SRLV, KMB, MSR, PAP, HKP, MSM,
527 and RVS. Writing of original draft – GCG. Manuscript review and editing - PAP, KMB, HKP, MSM,
528 and RVS. Funding acquisition – MSM, HKP, and RVS.

529 **ACKNOWLEDGEMENTS**

530 This study was supported by grants to HKP and RVS from the Council of Scientific and Industrial
531 Research (CSIR), Government of India (MLP0121 Phase-I and Phase-II) and the JC Bose Fellowship
532 of RVS granted by the Science and Engineering Research Board (SERB), Department of Science and
533 Technology, Government of India (GAP0444). We thank Dr. Rajkanwar Nathawat (Current address:
534 Yale University) for her guidance and suggestions on protein structure prediction analysis. We thank
535 the skilled workers at ICAR-IIRR and CSIR-CCMB for their support in field activities and
536 maintenance.

537 **CONFLICT OF INTEREST**

538 The authors declare that no conflict of interest exists.

539

540 **Supporting Information:**

541 **Table S1:** Statistics of the whole genome sequence data generated in this study.

542 **Table S2:** Statistics of the RNA sequence data generated in this study.

543 **Table S3:** Overlapping insect resistance QTL intervals

544 **Table S4:** Laccase-encoding genes that are situated in Chromosome 1 QTL interval.

545

546 **Figure S1:** Functional profiling of genes present in the QTL intervals and carrying SNPs.

547 **Figure S2:** Differential expression of genes in SM and SM92.

548 **Figure S3:** Differential regulation of phenylpropanoid pathway genes.

549 **Figure S4:** Enrichment of lignin metabolism related genes in the QTL intervals.

550 **Figure S5:** Differentially expressed lipid-related genes and their phylogeny.

551 **Figure S6:** Other significantly enriched pathways and corresponding differentially expressed genes.

552 **Figure S7:** Variation in the regulatory region of *OsLTPL146* in SM and SM92.

553 **Figure S8:** Multiple phenylpropanoid pathway metabolites are accumulated in SM and SM92.

554

555 **Data S1:** Phenotype scores of F2 progenies

556 **Data S2:** List of genes present in all the identified QTL intervals, the SNPs and their effects.

557 **Data S3:** List of genes predicted to harbor high effect causing SNPs in the QTL regions.

558 **Data S4:** List of SNPs selected as markers for trait association study using KASP assays.

559 **Data S5:** KASP assay information

560 **Data S6:** Genotype-phenotype information of screened F2 progenies

561 **Data S7:** Marker-Trait Association Analysis of F2 progenies

562 **Data S8:** Differentially expressed genes in SM upon YSB infestation at 72hpi (infested vs
563 uninfested)

564 **Data S9:** Differentially expressed genes in SM92 upon YSB infestation at 72hpi (infested vs
565 uninfested)

566 **Data S10:** List of differentially expressed genes that are located within the QTL intervals and their
567 log2 fold change values.

568 **Data S11:** Log2 fold change values of genes upregulated upon striped stem borer and yellow stem
569 borer in respective tolerant and susceptible lines

570 **Data S12:** Raw peak intensity data of metabolites

571 **Data S13:** Normalized peak intensity data of metabolites

572 **References:**

573 **Bentur JS, Padmakumari AP, Jhansilakshmi V, Padmavathi Ch, Kondala Rao Y, A.S. and P.I.**
574 (2011) *Insect resistance in Rice (2000-2009)*.,.

575 **Dobin, A., Davis, C.A., Schlesinger, F., Drenkow, J., Zaleski, C., Jha, S., Batut, P., Chaisson, M.**
576 **and Gingeras, T.R.** (2013) STAR: ultrafast universal RNA-seq aligner. *Bioinformatics*, **29**, 15–
577 21. Available at: <https://academic.oup.com/bioinformatics/article/29/1/15/272537> [Accessed
578 April 23, 2023].

579 **Dong, N.Q. and Lin, H.X.** (2021) Contribution of phenylpropanoid metabolism to plant development
580 and plant–environment interactions. *J. Integr. Plant Biol.*, **63**, 180–209. Available at:
581 <https://onlinelibrary.wiley.com/doi/full/10.1111/jipb.13054> [Accessed April 23, 2023].

582 **Fauth, M., Schweizer, P., Buchala, A., Markstädter, C., Riederer, M., Kato, T. and Kauss, H.**
583 (1998) Cutin Monomers and Surface Wax Constituents Elicit H₂O₂ in Conditioned Cucumber
584 Hypocotyl Segments and Enhance the Activity of Other H₂O₂ Elicitors. *Plant Physiol.*, **117**,
585 1373. Available at: [/pmc/articles/PMC34901/](https://pmc/articles/PMC34901/) [Accessed October 14, 2022].

586 **Franco, O.L., Rigden, D.J., Melo, F.R. and Grossi-de-Sá, M.F.** (2002) Plant α-amylase inhibitors
587 and their interaction with insect α-amylases. *Eur. J. Biochem.*, **269**, 397–412. Available at:
588 <https://onlinelibrary.wiley.com/doi/full/10.1046/j.0014-2956.2001.02656.x> [Accessed October
589 14, 2022].

590 **Gangwar, S.K., Chakraborty, S., Dasgupta, M.K. and Huda, A.K.S.** (1986) MODELLING
591 YIELD LOSS IN INDICA RICE IN FARMERS’ FIELDS DUE TO MULTIPLE PESTS.
592 *Ecosyst. Environ.*, **17**, 165–171.

593 **Gao, H., Ma, K., Ji, G., Pan, L. and Zhou, Q.** (2022) Lipid transfer proteins involved in plant–
594 pathogen interactions and their molecular mechanisms. *Mol. Plant Pathol.* Available at:
595 <https://onlinelibrary.wiley.com/doi/full/10.1111/mpp.13264> [Accessed October 13, 2022].

596 **Gesteiro, N., Butrón, A., Estévez, S. and Santiago, R.** (2021) Unraveling the role of maize (*Zea*
597 *mays* L.) cell-wall phenylpropanoids in stem-borer resistance. *Phytochemistry*, **185**, 112683.

598 **Goujon, M., McWilliam, H., Li, W., Valentin, F., Squizzato, S., Paern, J. and Lopez, R.** (2010)
599 A new bioinformatics analysis tools framework at EMBL–EBI. *Nucleic Acids Res.*, **38**, W695–
600 W699. Available at: https://academic.oup.com/nar/article/38/suppl_2/W695/1097251
601 [Accessed August 12, 2022].

602 **Gururaj Katti, Chitra Shanker, Padmakumari A.P., P.I.C.** (2011) Rice stem borers in India-
603 species composition and distribution. *Tech. Bull. No.59.*, 89.

604 **Heinrichs, Elvis & Medrano, F.G. and Rapusas, H.R.** (1985) *Genetic Evaluation for Insect*
605 *Resistance in Rice.*, Available at: http://books.irri.org/9711041103_content.Pdf.

606 **Holm, L.** (2022) Dali server: structural unification of protein families. *Nucleic Acids Res.*, **50**, W210–
607 W215. Available at: <https://academic.oup.com/nar/article/50/W1/W210/6591528> [Accessed
608 October 13, 2022].

609 **IRRI** (2014) *Standard evaluation system for rice. International Rice Research Institute*, Available at:
610 http://www.clrri.org/ver2/uploads/SES_5th_edition.pdf [Accessed July 31, 2020].

611 **Jena, K.K., Jeung, J.U., Lee, J.H., Choi, H.C. and Brar, D.S.** (2006) High-resolution mapping of
612 a new brown planthopper (BPH) resistance gene, Bph18(t), and marker-assisted selection for
613 BPH resistance in rice (*Oryza sativa* L.). *Theor. Appl. Genet.*, **112**, 288–297. Available at:
614 <https://link.springer.com/article/10.1007/s00122-005-0127-8> [Accessed July 1, 2022].

615 **Jumper, J., Evans, R., Pritzel, A., et al.** (2021) Highly accurate protein structure prediction with
616 AlphaFold. *Nat.* 2021 5967873, **596**, 583–589. Available at:
617 <https://www.nature.com/articles/s41586-021-03819-2> [Accessed October 14, 2022].

618 **Kawahara, Y., la Bastide, M. de, Hamilton, J.P., et al.** (2013) Improvement of the *oryza sativa*
619 nipponbare reference genome using next generation sequence and optical map data. *Rice*, **6**, 3–
620 10. Available at: <https://thericejournal.springeropen.com/articles/10.1186/1939-8433-6-4>
621 [Accessed August 12, 2022].

622 **Kim, T.H., Park, J.H., Kim, M.C. and Cho, S.H.** (2008) Cutin monomer induces expression of the
623 rice OsLTP5 lipid transfer protein gene. *J. Plant Physiol.*, **165**, 345–349. Available at:
624 <https://linkinghub.elsevier.com/retrieve/pii/S0176161707001162> [Accessed August 11, 2020].

625 **Kolattukudy, P.E., Rogers, L.M., Li, D., Hwang, C.S. and Flaishman, M.A.** (1995) Surface
626 signaling in pathogenesis. *Proc. Natl. Acad. Sci. U. S. A.*, **92**, 4080. Available at:
627 [/pmc/articles/PMC41890/?report=abstract](https://www.ncbi.nlm.nih.gov/pmc/articles/PMC41890/?report=abstract) [Accessed October 14, 2022].

628 **Krueger, F.** TrimGalore: A wrapper around Cutadapt and FastQC to consistently apply adapter and
629 quality trimming to FastQ files, with extra functionality for RRBS data. Available at:
630 <https://github.com/FelixKrueger/TrimGalore> [Accessed April 23, 2023].

631 **Lage, J.-L. Da** (2018) The Amylases of Insects. *Int. J. Insect Sci.*, **10**, 117954331880478. Available
22

632 at: [/pmc/articles/PMC6176531/](https://pmc/articles/PMC6176531/) [Accessed October 14, 2022].

633 **Lee, M.-H., Jeon, H.S., Kim, S.H., et al.** (2019) Lignin-based barrier restricts pathogens to the
634 infection site and confers resistance in plants. *EMBO J.*, **38**, e101948. Available at:
635 <https://onlinelibrary.wiley.com/doi/full/10.15252/embj.2019101948> [Accessed October 13,
636 2022].

637 **Letunic, I. and Bork, P.** (2021) Interactive Tree Of Life (iTOL) v5: an online tool for phylogenetic
638 tree display and annotation. *Nucleic Acids Res.*, **49**, W293–W296. Available at:
639 <https://academic.oup.com/nar/article/49/W1/W293/6246398> [Accessed August 12, 2022].

640 **Liao, Y., Smyth, G.K. and Shi, W.** (2014) featureCounts: an efficient general purpose program for
641 assigning sequence reads to genomic features. *Bioinformatics*, **30**, 923–930. Available at:
642 <https://academic.oup.com/bioinformatics/article/30/7/923/232889> [Accessed April 23, 2023].

643 **Love, M.I., Huber, W. and Anders, S.** (2014) Moderated estimation of fold change and dispersion
644 for RNA-seq data with DESeq2. *Genome Biol.*, **15**, 1–21. Available at:
645 <https://genomebiology.biomedcentral.com/articles/10.1186/s13059-014-0550-8> [Accessed
646 April 23, 2023].

647 **M.D. Pathak and Z.R.Khan** (1994) *Insect Pests of Rice*, International Rice Research Institute.
648 Available at: http://books.irri.org/9712200280_content.pdf [Accessed December 6, 2021].

649 **Magwene, P.M., Willis, J.H. and Kelly, J.K.** (2011) The Statistics of Bulk Segregant Analysis
650 Using Next Generation Sequencing. *PLOS Comput. Biol.*, **7**, e1002255. Available at:
651 <https://journals.plos.org/ploscompbiol/article?id=10.1371/journal.pcbi.1002255> [Accessed
652 October 23, 2022].

653 **Malvar, R.A., Butrón, A., Ordás, B. and Santiago, R.** (2008) Causes of natural resistance to stem
654 borers in maize. *Crop Prot. Res. Adv.*, **313**.

655 **Mansfeld, B.N. and Grumet, R.** (2018) QTLseqr: An R Package for Bulk Segregant Analysis with
656 Next-Generation Sequencing. *Plant Genome*, **11**, 180006. Available at:
657 <https://onlinelibrary.wiley.com/doi/10.3835/plantgenome2018.01.0006> [Accessed December
658 25, 2020].

659 **Miller, G.L.** (1959) Use of Dinitrosalicylic Acid Reagent for Determination of Reducing Sugar. *Anal. Chem.*, **31**, 426–428. Available at: <https://pubs.acs.org/doi/abs/10.1021/ac60147a030> [Accessed
660 August 29, 2023].

661

662 **Mirdita, M., Schütze, K., Moriwaki, Y., Heo, L., Ovchinnikov, S. and Steinegger, M.** (2022)
663 ColabFold: making protein folding accessible to all. *Nat. Methods* 2022 **19**, 679–682.
664 Available at: <https://www.nature.com/articles/s41592-022-01488-1> [Accessed August 12,
665 2022].

666 **Moin, M., Bakshi, A., Saha, A., Dutta, M., Madhav, S.M. and Kirti, P.B.** (2016) Rice ribosomal
667 protein large subunit genes and their spatio-temporal and stress regulation. *Front. Plant Sci.*, **7**,
668 1284.

669 **Muralidharan, K. and Pasalu, I.C.** (2006) Assessments of crop losses in rice ecosystems due to
670 stem borer damage (Lepidoptera: Pyralidae). *Crop Prot.*, **25**, 409417.

671 **Nagaraj, S., Senthil-Kumar, M., Ramu, V.S., Wang, K. and Mysore, K.S.** (2016) Plant ribosomal
672 proteins, RPL12 and RPL19, play a role in nonhost disease resistance against bacterial
673 pathogens. *Front. Plant Sci.*, **6**, 1192.

674 **Oliveros, J.C.** (2007) Venny. An interactive tool for comparing lists with Venn's diagrams. Available
675 at: <https://bioinfogp.cnb.csic.es/tools/venny/index.html>.

676 **Oneda, H., Lee, S. and Inouye, K.** (2004) Inhibitory Effect of 0.19 α -Amylase Inhibitor from Wheat
677 Kernel on the Activity of Porcine Pancreas α -Amylase and Its Thermal Stability. *J. Biochem.*,
678 **135**, 421–427. Available at: <https://academic.oup.com/jb/article/135/3/421/1072114> [Accessed
679 October 14, 2022].

680 **Padmakumari A.P, Seshu Madhav M, Uma Kanth B, Sunil B, Gopi, P, Karteek J, Laha GS,**
681 **Sundaram, RM , Subba Rao, LV, H.K.P. and R.S.** (2017) *EMS mutants as a novel source of*
682 *tolerance to yellow stem borer.*, Hyderabad.

683 **Padmakumari AP and Katti G** (2018) Designing insect bioassays for studying components of insect
684 pest management-rice yellow stem borer – as a case study. In *National Symposium*
685 *Entomology2018:Advances and Challenges*. Hyderabad, p. 117.

686 **Pang, Z., Chong, J., Zhou, G., et al.** (2021) MetaboAnalyst 5.0: narrowing the gap between raw
687 spectra and functional insights. *Nucleic Acids Res.*, **49**, W388–W396. Available at:
688 <https://academic.oup.com/nar/article/49/W1/W388/6279832> [Accessed April 23, 2023].

689 **Pathak, M.D.** (1977) DEFENSE OF THE RICE CROP AGAINST INSECT PESTS. *Ann. N. Y.*
690 *Acad. Sci.*, **287**, 287–295. Available at: <https://onlinelibrary.wiley.com/doi/full/10.1111/j.1749-6632.1977.tb34247.x> [Accessed December 6, 2021].

692 **Pathak, M.D.** (1968) Ecology of Common Insect Pests of Rice.
693 <http://dx.doi.org/10.1146/annurev.en.13.010168.001353>, **13**, 257–294. Available at:
694 <https://www.annualreviews.org/doi/abs/10.1146/annurev.en.13.010168.001353> [Accessed
695 December 6, 2021].

696 **Peltier, A.J., Hatfield, R.D. and Grau, C.R.** (2009) Soybean Stem Lignin Concentration Relates to
697 Resistance to Sclerotinia sclerotiorum. *Plant Dis.*, **93**, 149–154. Available at:
698 <https://pubmed.ncbi.nlm.nih.gov/30764097/> [Accessed October 13, 2022].

699 **Potupureddi, G., Balija, V., Ballichatla, S., et al.** (2021) Mutation resource of Samba Mahsuri
700 revealed the presence of high extent of variations among key traits for rice improvement. *PLoS
701 One*, **16**, e0258816. Available at:
702 <https://journals.plos.org/plosone/article?id=10.1371/journal.pone.0258816> [Accessed May 24,
703 2022].

704 **Quinlan, A.R. and Hall, I.M.** (2010) BEDTools: a flexible suite of utilities for comparing genomic
705 features. *Bioinformatics*, **26**, 841–842. Available at:
706 <https://academic.oup.com/bioinformatics/article/26/6/841/244688> [Accessed May 8, 2023].

707 **Ramu, V.S., Dawane, A., Lee, S., Oh, S., Lee, H.K., Sun, L., Senthil-Kumar, M. and Mysore,
708 K.S.** (2020) Ribosomal protein QM/RPL10 positively regulates defence and protein translation
709 mechanisms during nonhost disease resistance. *Mol. Plant Pathol.*, **21**, 1481–1494. Available
710 at: <https://onlinelibrary.wiley.com/doi/full/10.1111/mpp.12991> [Accessed October 14, 2022].

711 **Rubia, E.G., Heong, K.L., Zalucki, M., Gonzales, B. and Norton, G.A.** (1996) Mechanisms of
712 compensation of rice plants to yellow stem borer *Scirpophaga incertulas* (Walker) injury. *Crop
713 Prot.*, **15**, 335–340.

714 **Sakai, H., Lee, S.S., Tanaka, T., et al.** (2013) Rice Annotation Project Database (RAP-DB): an
715 integrative and interactive database for rice genomics. *Plant Cell Physiol.*, **54**. Available at:
716 <https://pubmed.ncbi.nlm.nih.gov/23299411/> [Accessed August 12, 2022].

717 **Salminen, T.A., Blomqvist, K. and Edqvist, J.** (2016) Lipid transfer proteins: classification,
718 nomenclature, structure, and function. *Planta*, **244**, 971–997. Available at:
719 <https://pubmed.ncbi.nlm.nih.gov/27562524/> [Accessed October 14, 2022].

720 **Santiago, R., Barros-Rios, J. and Malvar, R.A.** (2013) Impact of Cell Wall Composition on Maize
721 Resistance to Pests and Diseases. *Int. J. Mol. Sci. 2013, Vol. 14, Pages 6960-6980*, **14**, 6960–

722 6980. Available at: <https://www.mdpi.com/1422-0067/14/4/6960/htm> [Accessed October 13,
723 2022].

724 **Santos, R.B., Nascimento, R., Coelho, A. V. and Figueiredo, A.** (2020) Grapevine–Downy Mildew
725 Rendezvous: Proteome Analysis of the First Hours of an Incompatible Interaction. *Plants* **2020**,
726 *Vol. 9, Page 1498*, **9**, 1498. Available at: <https://www.mdpi.com/2223-7747/9/11/1498/htm>
727 [Accessed October 14, 2022].

728 **Savary, S., Willocquet, L., Pethybridge, S.J., Esker, P., McRoberts, N. and Nelson, A.** (2019)
729 The global burden of pathogens and pests on major food crops. *Nat. Ecol. Evol.*, **3**, 430–439.
730 Available at: <https://www.nature.com/articles/s41559-018-0793-y>.

731 **Schweizer, P., Jeanguenat, A., Whitacre, D., Métraux, J.P. and Mössinger, E.** (1996) Induction of
732 resistance in barley against *Erysiphe graminis*f.sp.*hordeib*y free cutin monomers. *Physiol. Mol.*
733 *Plant Pathol.*, **49**, 103–120.

734 **Selvaraju, K., Shanmugasundaram, P., Mohankumar, S., Asaithambi, M. and Balasaraswathi,**
735 **R.** (2007) Detection of quantitative trait locus for leaffolder (*Cnaphalocrocis medinalis*
736 (Guenée)) resistance in rice on linkage group 1 based on damage score and flag leaf width.
737 *Euphytica*, **157**, 35–43. Available at: <https://link.springer.com/article/10.1007/s10681-007-9394-6> [Accessed July 1, 2022].

739 **Sievers, F., Wilm, A., Dineen, D., et al.** (2011) Fast, scalable generation of high-quality protein
740 multiple sequence alignments using Clustal Omega. *Mol. Syst. Biol.*, **7**, 539. Available at:
741 <https://onlinelibrary.wiley.com/doi/full/10.1038/msb.2011.75> [Accessed August 12, 2022].

742 **Su, J., Zhang, Z., Wu, M. and Gao, C.** (2014) Geographic susceptibility of *Chilo suppressalis*
743 Walker (Lepidoptera: Crambidae), to chlorantraniliprole in China. *Pest Manag. Sci.*, **70**, 989–
744 995. Available at: <https://onlinelibrary.wiley.com/doi/full/10.1002/ps.3640> [Accessed October
745 13, 2022].

746 **Sun, L., Su, C., Wang, C., Zhai, H. and Wan, J.** (2005) Mapping of a Major Resistance Gene to
747 the Brown Planthopper in the Rice Cultivar Rathu Heenati. *Breed. Sci.*, **55**, 391–396. Available
748 at: <http://www.> [Accessed July 1, 2022].

749 **Tae, H.K., Moon, C.K., Jong, H.P., Seong, S.H., Byung, R.K., Byoung, Y.M., Mi, C.S. and Sung,**
750 **H.C.** (2006) Differential expression of rice lipid transfer protein gene(LTP) classes in response
751 to abscisic acid, salt, salicylic acid, and the fungal pathogen *Magnaporthe grisea*. *J. Plant Biol.*

752 2006 495, **49**, 371–375. Available at: <https://link.springer.com/article/10.1007/BF03178814>
753 [Accessed October 14, 2022].

754 **Takagi, H., Abe, A., Yoshida, K., et al.** (2013) QTL-seq: Rapid mapping of quantitative trait loci in
755 rice by whole genome resequencing of DNA from two bulked populations. *Plant J.*, **74**, 174–
756 183. Available at: <https://onlinelibrary.wiley.com/doi/full/10.1111/tpj.12105> [Accessed July 29,
757 2020].

758 **Thimm, O., Bläsing, O., Gibon, Y., et al.** (2004) MAPMAN: a user-driven tool to display genomics
759 data sets onto diagrams of metabolic pathways and other biological processes. *Plant J.*, **37**, 914–
760 939. Available at: <https://pubmed.ncbi.nlm.nih.gov/14996223/> [Accessed April 23, 2023].

761 **Trautmann, H.S. and Ramsey, K.M.** (2022) A Ribosomal Protein Homolog Governs Gene
762 Expression and Virulence in a Bacterial Pathogen. *J. Bacteriol.* Available at:
763 <https://journals.asm.org/doi/10.1128/jb.00268-22> [Accessed October 14, 2022].

764 **Wang, Y., Ju, D., Yang, X., Ma, D. and Wang, X.** (2018) Comparative Transcriptome Analysis
765 Between Resistant and Susceptible Rice Cultivars Responding to Striped Stem Borer (SSB),
766 Chilo suppressalis (Walker) Infestation. *Front. Physiol.*, **9**, 1717.

767 **Warner, J.R. and McIntosh, K.B.** (2009) How Common Are Extraribosomal Functions of
768 Ribosomal Proteins? *Mol. Cell*, **34**, 3–11.

769 **Weisberg, R.A.** (2008) Transcription by Moonlight: Structural Basis of an Extraribosomal Activity
770 of Ribosomal Protein S10. *Mol. Cell*, **32**, 747–748.

771 **Wool, I.G.** (1996) Extraribosomal functions of ribosomal proteins. *Trends Biochem. Sci.*, **21**, 164–
772 165.

773 **Yu, Y., Xing, Y., Liu, F., Zhang, X., Li, X., Zhang, J. and Sun, X.** (2021) The Laccase Gene Family
774 Mediate Multi-Perspective Trade-Offs during Tea Plant (*Camellia sinensis*) Development and
775 Defense Processes. *Int. J. Mol. Sci.* 2021, Vol. 22, Page 12554, **22**, 12554. Available at:
776 <https://www.mdpi.com/1422-0067/22/22/12554/htm> [Accessed October 13, 2022].

777 **Zhao, Q., Nakashima, J., Chen, F., et al.** (2013) LACCASE Is Necessary and Nonredundant with
778 PEROXIDASE for Lignin Polymerization during Vascular Development in *Arabidopsis*. *Plant*
779 *Cell*, **25**, 3976. Available at: [/pmc/articles/PMC3877815/](https://pmc/articles/PMC3877815/) [Accessed October 13, 2022].

780

781
782

Table 1: List of the putative QTL predicted to be associated with YSB tolerance. SNPs - Single Nucleotide Polymorphisms; Q-val - False Discovery Rate.

S.No.	Chromosome	Start ^a	End ^b	Length ^c	Number of SNPs ^d	Mean Q-val ^a
1	1	33465932	36594124	3128192	741	0.025
2		37253341	37887039	633698	166	0.033
3	5	1931441	2666236	734795	268	0.030
4		3360636	3839012	478376	134	0.042
5	7	2039475	2340432	300957	94	0.035
6	10	21348600	22786612	1438012	719	0.013
7	12	7703041	10065030	2361989	1979	0.034
8		16700754	18048717	1347963	1026	0.030
9		19115124	19867810	752686	825	0.043
10		22145804	23226149	1080345	529	0.031

784 Beginning of the mapped QTL interval

785 ^b End of the mapped QTL interval

786 ^c Length of the mapped QTL interval in base pairs

787 ^d Number of SNPs situated in the mapped QTL interval

788

789 **Table 2:** Markers that are significantly associated with YSB tolerance.

Marker	Chromosome	Position	REF ^a	ALT ^b	SNP-index Tol ^c	SNP-index Sus ^d	Delta SNP-index	P	% PVE	Gene ID	Description
S2	1	33886610	C	G	0	0.61	-0.61	0.034	5.7	Os01g0800266	Similar to Phosphoglycerate kinase. (Os01t0800266-00)
S3		33957364	G	A	0.29	0.62	-0.33	0.022	6.7	Os01g0801700	Ribosomal protein S35, mitochondrial domain containing protein. (Os01t0801700-01)
S5		34710185	G	A	0	0.63	-0.63	0.007	9.2	Os01g0816400	Similar to microtubule organization protein. (Os01t0816400-01)
S6		35088627	C	T	0	0.69	-0.69	0.019	7.1	Non-exonic [†]	-
S17	5	2366109	G	A	0.65	0	0.65	0.047	5.0	Os05g0141200	Hypothetical conserved gene. (Os05t0141200-00)
S18		3157367	C	T	0.59	0	0.59	0.033	5.8	Non-exonic	-
S19		3743040	G	T	0.91	0	0.91	0.022	6.6	Non-exonic	-
S20		4321188	C	T	0.66	0	0.66	0.047	5.1	Os05g0172300	Domain of unknown function DUF632 domain containing protein. (Os05t0172300-01)
S28	10	21786052	C	T	0.73	0	0.73	0.017	7.2	Non-exonic	-
S29		21853916	T	A	0.82	0	0.82	0.017	7.2	Non-exonic	-
S30		21955122	C	T	0.68	0	0.68	0.017	7.2	Os10g0557800	Conserved hypothetical protein. (Os10t0557800-01)
S31		21955776	T	A	0.76	0.45	0.31	0.038	5.5	Os10g0557900	Peptidase M10A and M12B, matrixin and adamalysin family protein. (Os10t0557900-00)
S32		21965877	C	G	0.69	0.38	0.31	0.017	7.2	Os10g0558125	Similar to Matrixin family protein, expressed. (Os10t0558125-00)
S45	12	18013596	A	T	0.63	0	0.63	0.034	5.8	Non-exonic	-

790

791 ^a Allele present in the wildtype line

792 ^b Allele present in the mutant line

793 ^c SNP-index of the tolerant bulk

794 ^d SNP-index of the susceptible bulk

795 * Control – SNPs from genomic regions outside QTL intervals

796 [†] Non-exonic – SNPs from the QTL intervals that are not exonic

797 %PVE - % Phenotypic Variation Explained

798

799 **Figure 1**

800 **SM92 exhibited a high level of tolerance to YSB infestation.** (A) Field screening with YSB larvae
801 revealed an increased incidence of dead hearts in SM as compared to SM92. (B) Violin plot showing
802 the number of live and dead YSB larvae in the infested stems of SM and SM92. The number of live
803 larvae were significantly less in the stems of SM92 as compared to SM. Asterisk indicates *P*-value of
804 less than 0.05 as calculated using a 2-way ANOVA test. (C) and (D) Images indicating the presence
805 of a live larvae in SM and a dead larva in SM92, respectively. Black arrowheads denote the larvae.

806 **Figure 2**

807 **Mapping genomic loci associated with YSB tolerance in F2 population using BSA-QTL-seq.** (A)
808 Phenotype scores of the F₂ population consisting of 314 progenies followed a continuous distribution
809 suggesting the quantitative nature of YSB tolerance. The green bar indicates progenies that
810 constituted tolerant bulk (n=21) and the red bars indicate the progenies that constituted susceptible
811 bulk (n=24). (B) Delta SNP-index plot generated by the QTL-seq pipeline shows two genomic loci
812 (red arrowheads) that could be linked to YSB tolerance. The red, green, and blue lines represent the
813 confidence intervals at 90%, 95%, and 99%, respectively. (C) G' plot generated by the QTL-seq
814 pipeline shows additional genomic loci (blue arrowheads) that might be associated with YSB
815 tolerance. The red line represents the *q*-value cut-off of 0.05. The black line in (B) and (C) represents
816 the moving average line calculated using a window size of 500kb.

817 **Figure 3**

818 **Transcriptome profiling revealed putative rice functions associated with YSB tolerance.** (A) Bar
819 chart depicting the number of differentially expressed genes in SM and SM92 upon YSB infestation
820 in comparison to uninfested samples, as obtained through RNA-sequencing based transcriptome
821 profiling of stem samples at 72 hours post infestation. (B) Venn diagram comparing the differentially
822 expressed genes in SM and SM92. (C) and (D) Gene enrichment analysis showing the upregulated
823 pathways in SM and SM92 post YSB infestation.

824 **Figure 4**

825 **Comparative transcriptome indicated a possible candidate gene for YSB tolerance.** (A) Venn
826 diagram showing the comparison of genes upregulated in rice lines that are tolerant to striped stem
827 borer (SSB) from Wang et al (2018) and yellow stem borer (YSB). The intersection indicates 527
828 genes that are commonly upregulated. (B) Gene enrichment analysis of the stem borers-induced genes

829 revealed the enrichment of functions involved in alpha-amylase inhibition, glycoproteins, and
830 secreted proteins. (C) Expression of the gene *OsLTPL16* was observed to be upregulated by SSB and
831 YSB in tolerant rice lines and downregulated in susceptible rice lines. (D) Structure prediction and
832 homology search suggests that *OsLTPL146* might encode an alpha-amylase inhibitor. Structure
833 model of OsLTPL146 is colored green and the solved structure of wheat alpha-amylase inhibitor
834 (PDB:1hss) is colored brown.

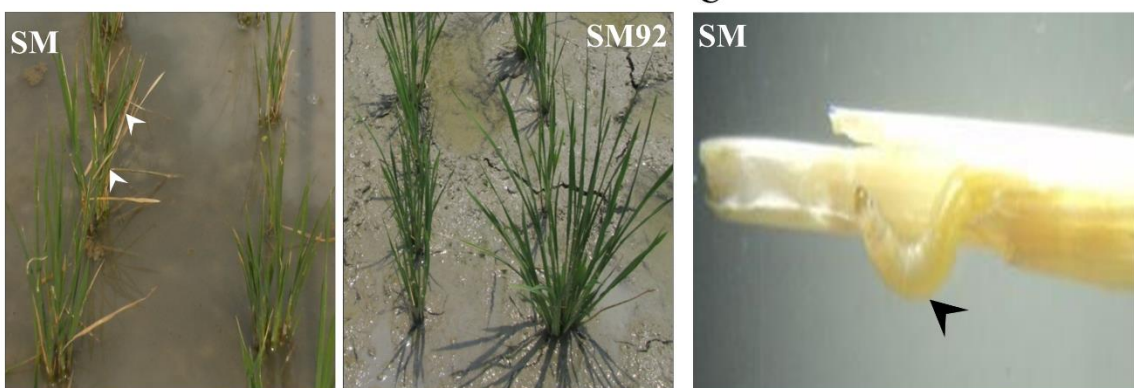
835 **Figure 5**

836 **YSB infestation causes considerable changes in the plant metabolite composition.** (A) Principal
837 Component Analysis (PCA) plot showing the clustering of SM and SM92 samples infested with YSB
838 (pink- and purple-shaded oval) indicating an overlapping response in both SM and SM92. The
839 uninfested samples, however, showed a loose clustering, probably indicating differences in the basal
840 metabolite composition. (B) Box plot showing the normalized intensity of certain phenylpropanoid
841 pathway metabolites in SM and SM92 upon YSB infestation and uninfested conditions. *P*-values
842 were calculated using unpaired t-test with multiple comparison correction using Holm-Sidak method.
843 *P*<0.05 is considered to be statistically significant.

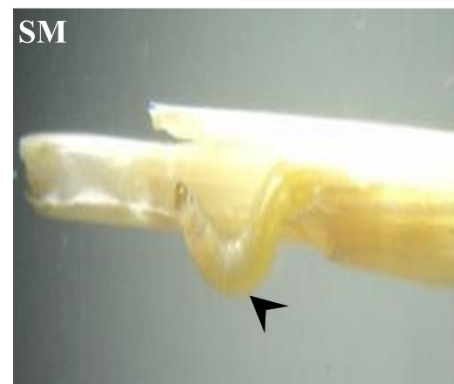
844

845

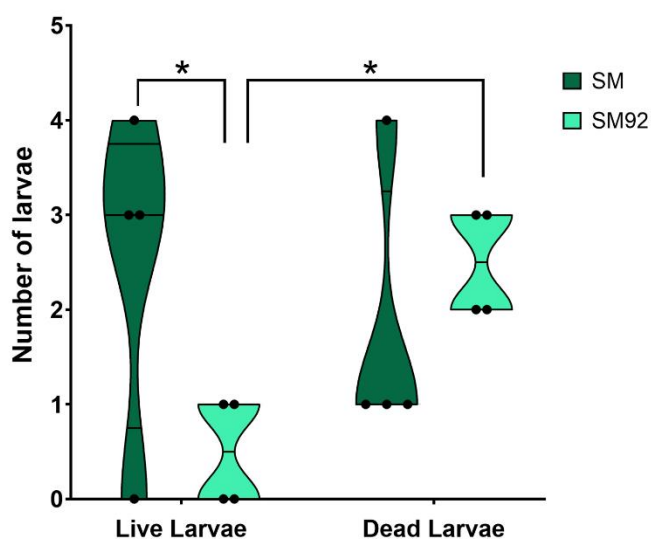
A



C



B



D

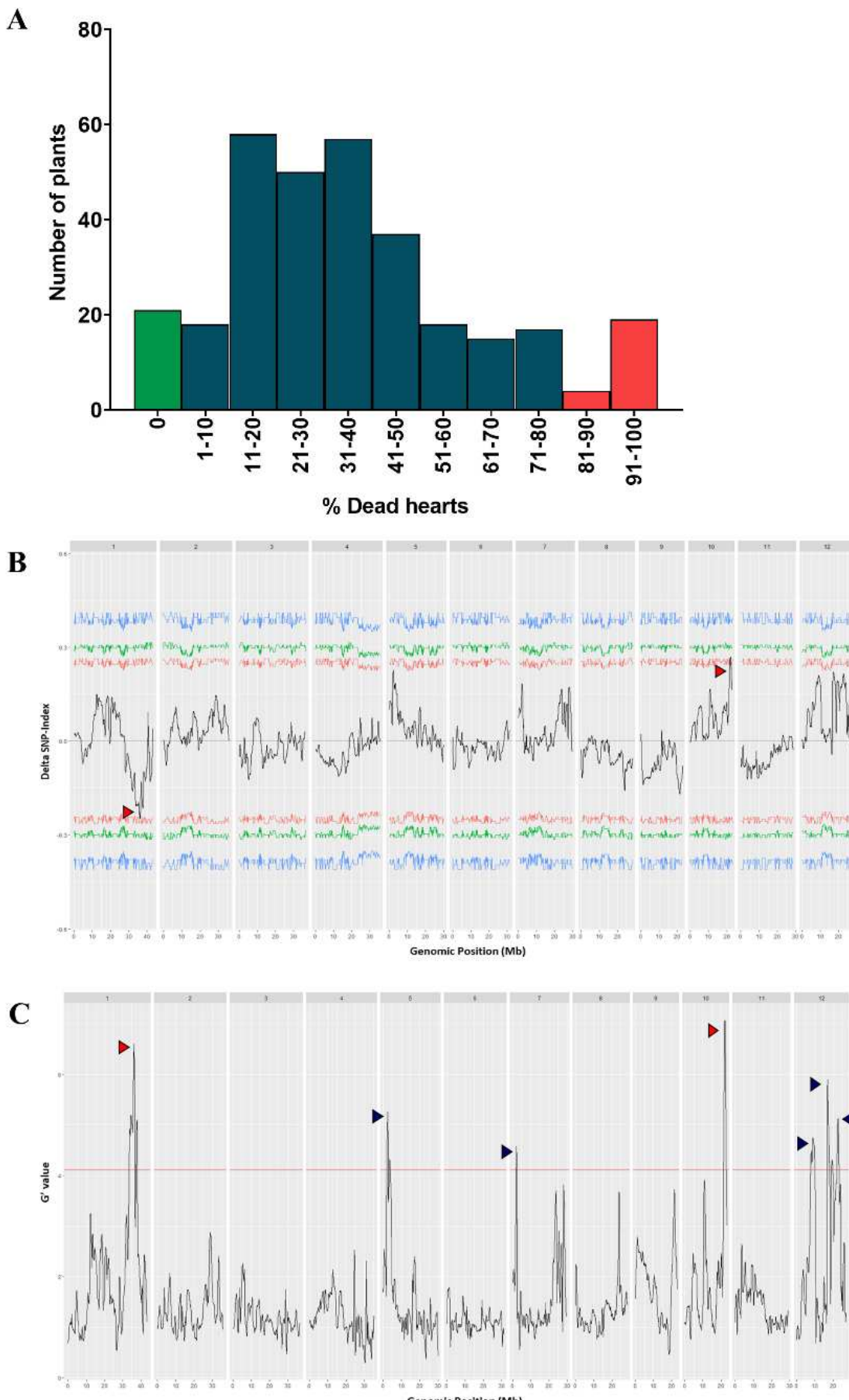


860

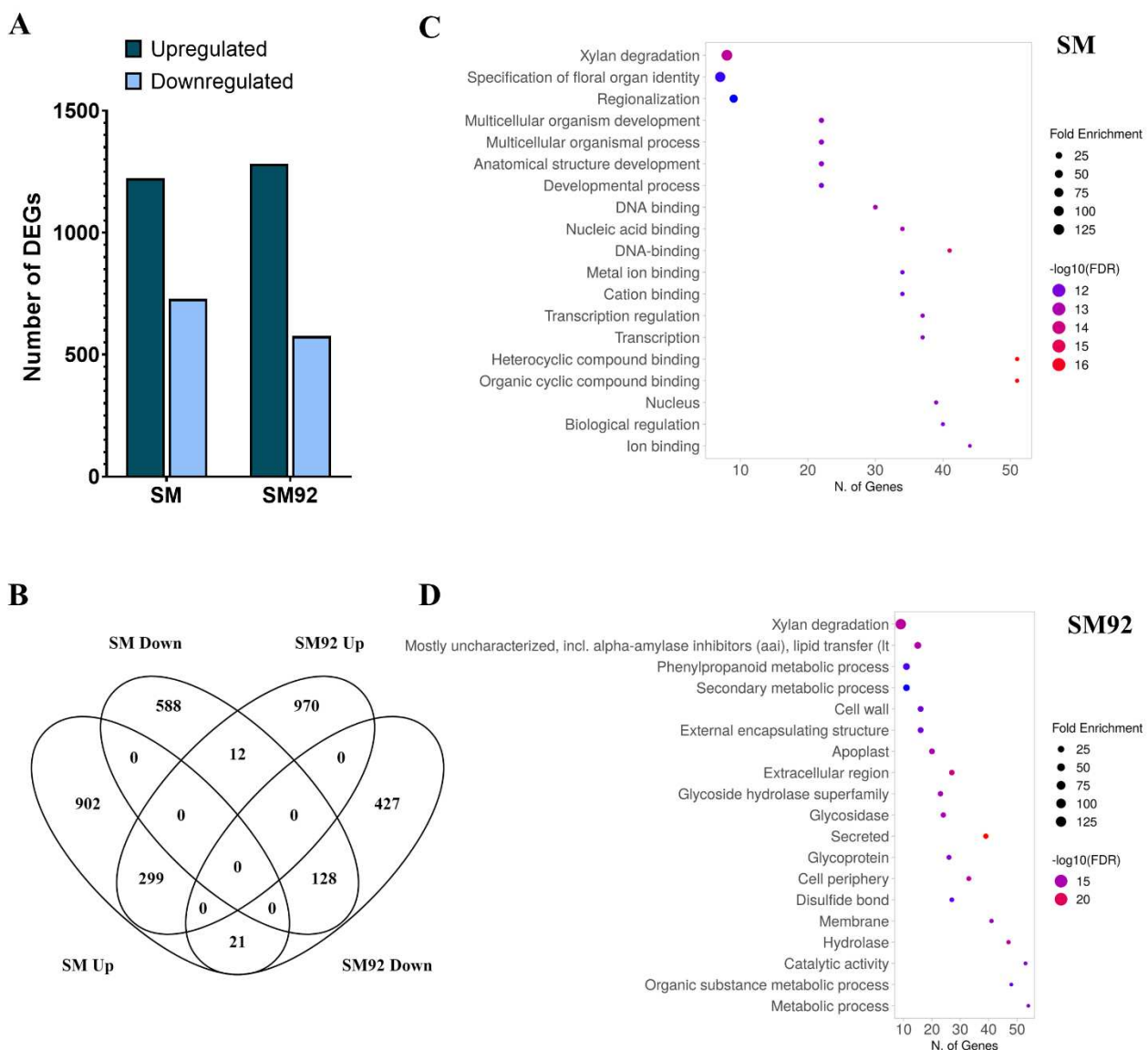
861

32

862

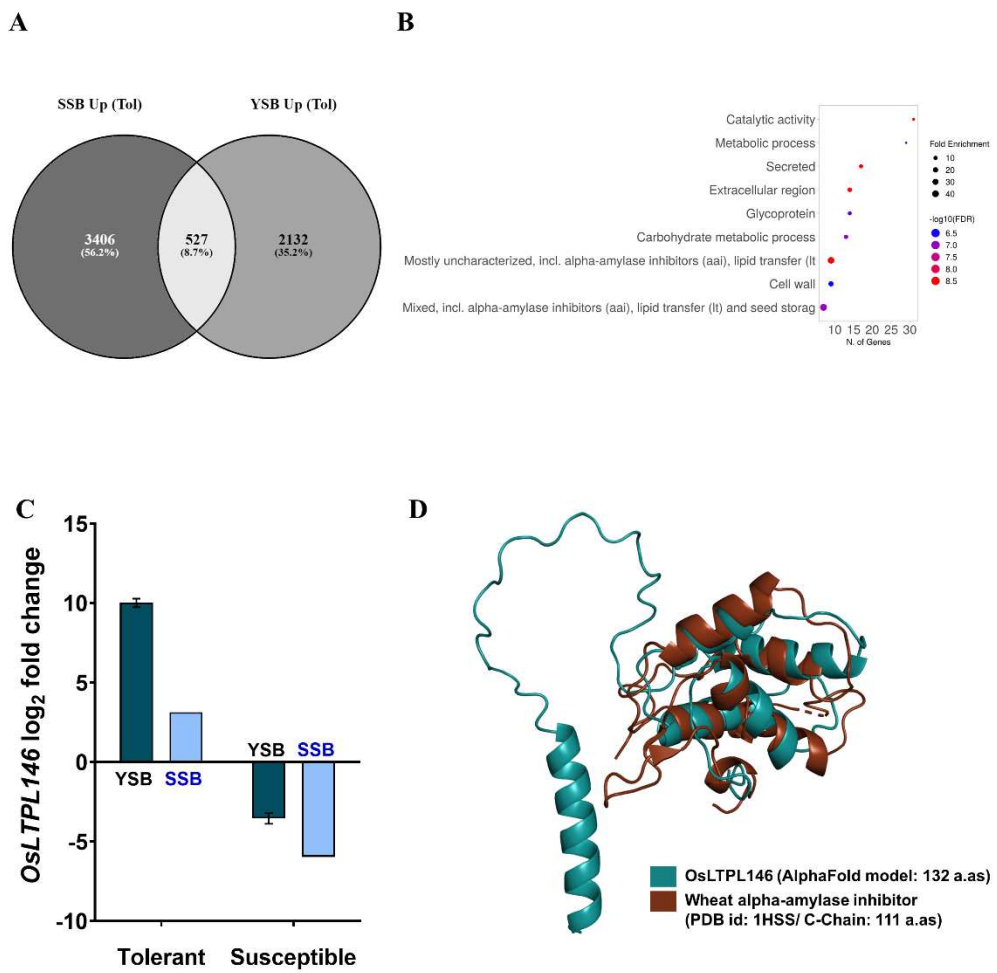


863

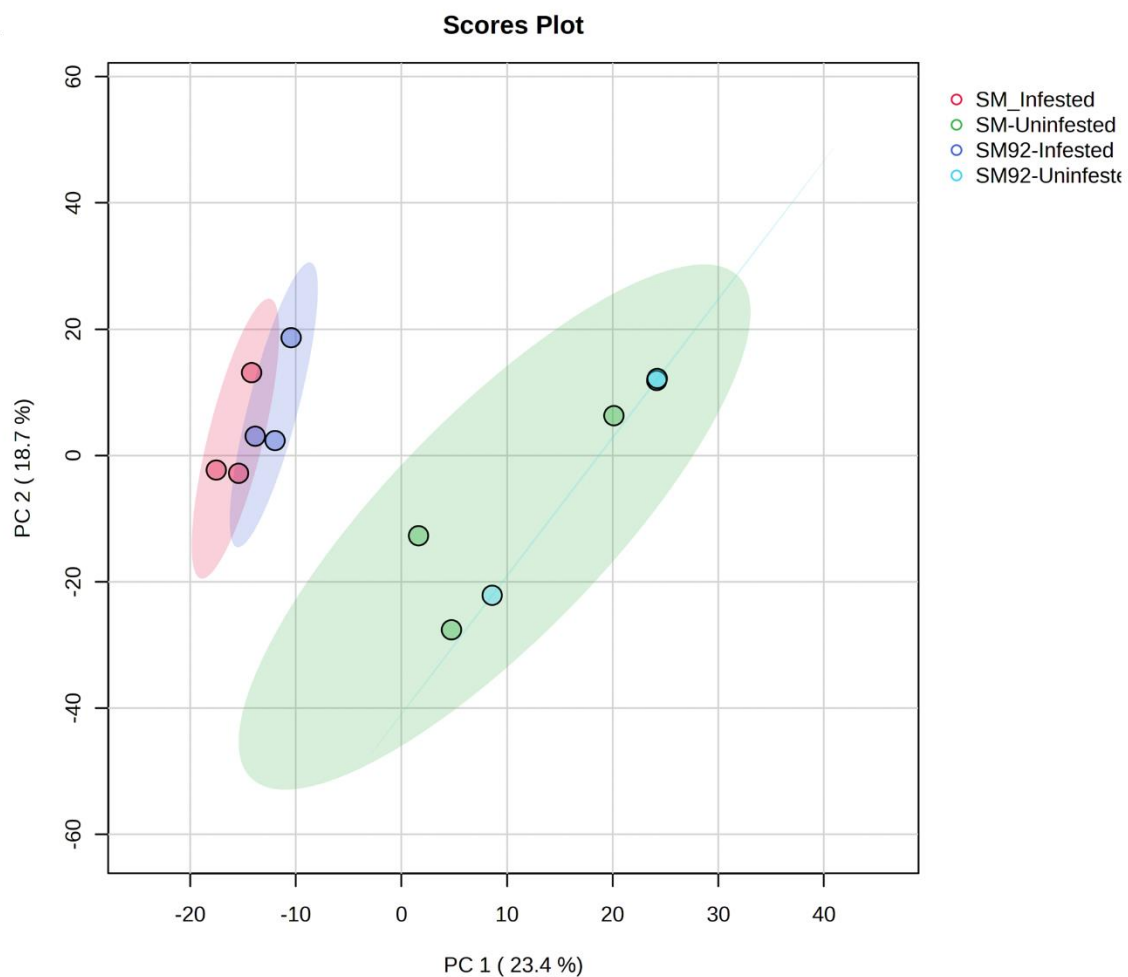


864

34



A



B

